Solution-Processed Infrared Photovoltaic Devices

Dean D. MacNeil and Edward H. Sargent
Department of Electrical and Computer Engineering
University of Toronto
Toronto, Ontario, M5S 3G4, Canada
1-416-978-8935
dean.macneil@utoronto.ca

ABSTRACT
Physically flexible, solution-processed solar cells have the potential to harvest light conveniently, cheaply and efficiently. Absorption of the considerable power in the infrared region of the solar spectrum is necessary for efficient solution-processed solar cells. We use lead sulphide (PbS) colloidal nanoparticles (quantum dots) that are quantum size effect tunable, allowing tailoring of absorption onset between 900 and 2000 nm. A number of device architectures will be described within, leading to photovoltaic devices which exhibit external quantum efficiencies exceeding 1%.

Categories and Subject Descriptors
A General Literature

A.0 General

General Terms: Performance

Keywords: Quantum dots, Photovoltaics, Solution-processing, Infrared, Nanocrystals

1. INTRODUCTION
One of the major obstacles to the wide-spread adoption of photovoltaics is the high cost of conventional silicon based solar cells. Consequently, large-area, solution-processed photovoltaic devices fabricated from materials other than crystalline silicon are of keen interest to the energy community. In addition to large-area devices these solution processed photovoltaics could fill niche applications related to portable power for electronics and communication. Research in this area is carried out with the goal that it will lead to the realization of solar cells which can serve as viable alternatives to silicon based devices, but at a fraction of the cost.

Our group works with colloidal quantum dots, nanoparticles that are produced in, and processed from, solution. They can be conveniently coated onto nearly anything – a window, a wall, a piece of fabric. Compared to the semiconductors traditionally used to make photovoltaics, they are cheap, offer lower equipment needs, and easy to produce. Solution processing opens up the use of a variety of techniques such as spin-coating, printing and spraying while traditional silicon solar cell methods (epitaxy) are limited in the type of precursors, high material and equipment cost, and harsh conditions. There is an increased desire to produce large-area photovoltaics with physical flexibility based on plastic materials. The use of sensitizing conjugated polymers has addressed these issues, but the best power conversion efficiencies have been limited to about 3% [1,2,3]. Some of the issues limiting the efficiencies are the incomplete overlap of the absorption spectrum of the polymers with the sun's power spectrum, as well as the limited efficiency in separating and extracting charge carriers.

Typical research in polymer photovotaics has been limited to wavelengths shorter than 750 nm. We focus our attention as a result on the largely untapped infrared region of the spectrum, since half of the sun's power spectrum lies beyond 700 nm. Sensitizing conjugated polymers with infrared-active nanocrystal quantum dots provides a spectrally tunable means of accessing the infrared while maintaining the advantageous properties of polymers. Here, we will report on two device architectures using a variety of polymers and quantum-size-effect-tuned lead sulfide (PbS) to obtain absorption in the infrared between 900 and 2000 nm [4].

The devices described within could be incorporated into a number of device applications. This include compatibility with existing Si solar cells, but by converting a portion of the spectrum that is inaccessible to traditional silicon technology one can increase the overall power conversion efficiency of the cell. Perhaps a standalone application may be viable, but efficiencies need to be increased to the point of commercial viability. A third application is in the area of thermal-photovotaics, where one converts thermal radiation, such as waste heat from industrial manufacturing processes, into usable electrical energy. Since the predominant emission wavelength in the field of thermal photovotaics lie in the range of 1-3 um, the nanocrystals devices used herein lead naturally to applications in thermal photovoltaics. Finally, one can envision our PbS nanocrystals as the bottom layer (due to its band gap) of an all organic multi-junction photovoltaic devices.

2. Experimental
2.1 PbS Synthesis and Processing
The synthesis procedure has been described previously in the literature [5]. Briefly, PbO is dissolved in oleic acid and heated to 150°C. Bis(trimethylsilyl)-sulfide (TMS) in octadecene is added to the lead oleate solution. Nucleation occurs and the temperature is kept at the desired growth temperature. The size of the nanocrystals are controlled by varying the concentration of the capping ligand; the injection temperature and time; the growth temperature and time; and the ratio of oleic acid to sulfur to lead. When the nanocrystals reach the desired size they are precipitated

DAC 2006, July 24-28, 2006, San Francisco, California, USA.

by the addition of a polar solvent and can be redispersed using a non-polar solvent.

As synthesized nanocrystals contain large oleate ligands that are know to be insulating. To improve the electrical properties of our nanocrystals, a ligand exchange procedure to shorter ligands is performed. As synthesized nanocrystals are precipitated and then redispersed in an excess of the new ligands (octylamine, butylamine). After a few days the oleate ligands have been exchanged for new shorter amine ligands.

2.2 Device Processing

In this paper we will concentrate on two devices, one will be referred to as the blend device, the other as the layered device.

The blend device consisted of a 40 nm poly(p-phenylenevinylene) (PPV) hole transport layer spin-coated on an ITO-coated glass slide and annealed at 200°C for 3 hours in vacuum. A poly[2-methoxy-5-(2'-ethylhexyloxy-p-phenylenevinylene)] (MEH-PPV)/PbS blend (90% nanocrystal by weight) in chloroform was then spin-coated on the PPV layer to a thickness of 100-150 nm. Upper contacts were deposited by thermal evaporation 150 nm of Mg followed by 50 nm of Au. More information can be found in [6].

The layered device consisted of a 40 nm poly(3,4-ethylenedioxythiophene) (PEDOT): poly(styrenesulfonate) (PSS) spin-coated on an ITO-coated glass slide and annealed at 120°C for 30 min in vacuum. In a N_2 filled glove box, an 80 nm poly(3-octyl-thiophene) (P3OT) layer was then spin-coated from chlorobenzene and annealed for 4 min at 140°C. A PbS solution in hexane was spin-coated on top of the P3OT to various thicknesses. The top contacts were prepared by thermal evaporation of 80 nm of Al followed by 150 nm of Ag. More information can be found in [7].

Devices were tested using an Agilent 4155C Semiconductor Parameter Analyzer and microprobe station. The optical excitation was provided by a 975 nm continuous-wave semiconductor laser, which allowed for selective excitation of the nanocrystal phase. More information can be found in [6,7].

3. Results and Discussion

3.1 Blend Device

The device structure is described in section 2.2. The PPV layer serves as a hole transport layer as well as providing a smooth, pinhole-free layer to cast the film which eliminates shorts. More importantly, it decreases the dark current through the introduction of a injection barrier that allows larger ratios of photocurrent to dark current. Unfortunately, the PPV layer reduces the photocurrent internal quantum efficiency due to the generation of a barrier to extraction of photogenerated holes (reverse bias) and electrons (forward bias).

Figure 1 shows the dark current and photocurrent curves near zero bias at various incident powers and demonstrates the presence of a photovoltaic effect under continuous-wave illumination at 975 nm. The photocurrent I-V curves show diode-like behaviour, with higher photocurrents in the reverse bias, giving a ratio of photocurrent to dark current at -5V bias of over 600. The asymmetry in I-V curves is due to the work-function difference between ITO, PPV, and Mg as can be seen in the band diagram in the insert of Figure 1.

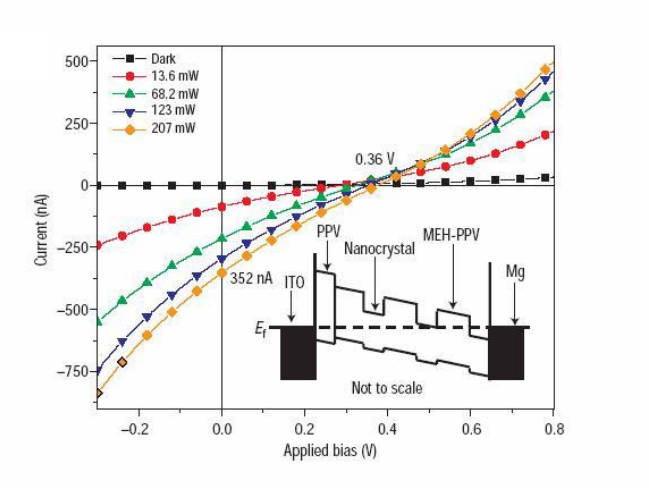

Figure 1. Dark current and photocurrent near zero bias. Proposed band diagram under equilibrium.

After excitation by a photon, an electron in the valence band of the nanocrystal is transferred to the conduction band, while the hole in the valence band may transfer to the hole-conducting MEH-PPV and the electron can either remain in the nanocrystal or move through the nanocrystal network by hopping or tunneling. This suggests a type II heterostructure.

The maximum short-circuit current from Figure 1 is 350 nA for an incident power of 207 mW, while the open-circuit voltage is 0.36V. The internal quantum efficiency is defined as the ratio of the number of collected charges to the number of absorbed photons at the pump wavelength. At an incident power of 2.7 mW the internal quantum efficiency is about 3%. At a short-circuit current of 350 nA the short-circuit internal quantum efficiency is ~0.006%. By varying the size of the nanocrystals during processing, photocurrent spectra were demonstrated (Figure 2) with peaks tailored to 980 nm, 1.200 um and 1.355 um.

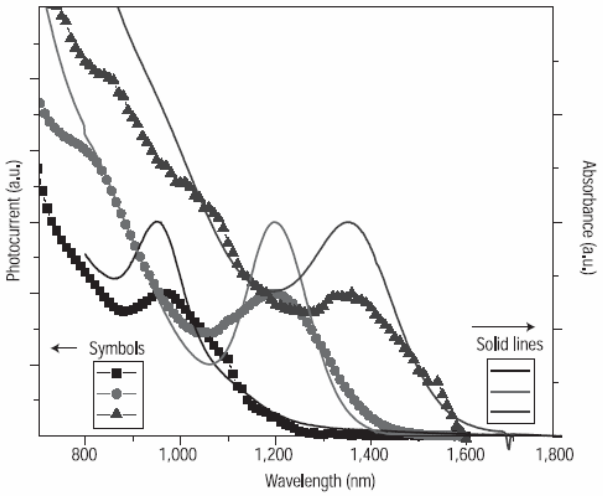

Figure 2. Photocurrent spectral response (symbols) and the corresponding absorption spectra (solid lines) for three different samples.

3.2 Layered Device

The device structure is described in section 2.2. Here the infrared-absorbing active layer is based purely on semiconductor nanoparticles with no semiconductor polymer matrix.

The goal of this device structure was to increase the quantum efficiencies of the IR solar cells. The performance of the device in section 3.1 suffered from poor charge carrier extraction due to its poor fill factor, large difference in quantum efficiency under bias versus open circuit conditions as well as rapid saturation in efficiency with increased incident power. These have been addressed here by the new device architecture and the use of shorter organic ligands to passivate the nanoparticles surface.

Four devices were fabricated, device A through C as described in section 2.2, but had different thicknesses of active nanocrystal (NC) layer. Device D had no P3OT layer deposited, thus the 160 nm nanocrystal layer was deposited directly on top of PEDOT:PSS. Table 1 summarizes the structure and performance of each device. For device A through C, the short-circuit current increased monotonically as the thickness of the nanocrystal layer was increased. The importance of the P3OT layer is seen when comparing device A to D, it is clear that the P3OT layer increases the open circuit voltage of the device while the fill factor and short-circuit current remains similar.

Table 1. Device Performance at 1260 nm and 166uW illumination

Device	Description	NC thickness (nm)	Fill Factor	Voc (V)	Isc (uA)
A	P3OT/NC bilayer	160	0.32	0.26	0.51
B	P3OT/NC bilayer	115	0.3	0.12	0.46
C	P3OT/NC bilayer	80	0.4	0.02	0.16
D	No P3OT	160	0.28	0.14	0.73

Table 2 presents the internal and external quantum efficiencies for device A to D. These devices have shown more than a 600 fold increase in efficiency over the devices described in section 3.1.

Table 2. Quantum efficiencies of devices A-D

Device	IQE (%)	EQE (%)
A	5.2	1.1
B	11.3	1.8
C	5.5	0.6
D	6.4	1.4

These two novel device architectures have shown that we have been able to achieve efficient solution-cast infrared photovoltaic devices beyond 1 um. The best devices presented herein exhibit external quantum efficiencies exceeding 1% corresponding to internal quantum efficiency greater than 10%.

4. ACKNOWLEDGMENTS

We thank the numerous members of our group that have contributed to these results; S.A. McDonald, .G. Konstantatos, S. Zhang, P.W. Cyr, E.J.D. Klem, L.Levina, A. Maria.

5. REFERENCES

[1] Granstrom, M., Petritsch, K., Arias, A.C., Lux, A., Andersson, M.R., and Friend, R.H., Laminated fabrication of polymeric photovoltaic diodes. *Nature*, *395*, 1998, 257-260.

[2] Huynh, W.U., Dittmer, J.J., and Alivisatos, A.P., Hybrid nanorod-polymer solar cells. *Science*, *295*, 2002, 2425-2428.

[3] Padinger, F., Rittberger, R.S., and Sariciftci, N.S., Effects of postproduction treatment on plastic solar cells, *Adv. Funct. Mater.*, *13*, 2003, 85-88.

[4] Sargent, E.H., Infrared Quantum Dots. *Adv. Mater., 17*, 2005, 515-522.

[5] Hines, M.A., and Scholes, G.D., Colloidal PbS nanocrystals with size-tunable near-infrared emission: observation of post synthesis self-narrowing of the particle size distribution. *Adv. Mater., 15,* 2003, 1844-1849.

[6] McDonald, S.A., Konstantatos, G., Zhang, S., Cyr, P.W., Klem, E.J.D., Levina, L., Sargent, E.H., Solution-processed PbS quantum dot infrared photodetectors and photovoltaics, *Nature Materials, 4,* 2005, 138-142.

[7] Maria, A., Cyr, P.W, Klem, E.J.D., Levina, L., Sargent, E.H., Solution-processed infrared photovoltaics with >10% monochromatic internal quantum efficiency, *App. Phys. Lett., 87*, 2005, 213112-3